J. Appl. Comput. Mech., 6(4) (2020) 813-822
DOI: 10.22055/JACM.2019.29929.1664

ISSN: 2383-4536
jacm.scu.ac.ir

M&MoCS

Shahid Chamran University of Ahvaz

Journal of Applied and Computational Mechanics

Research Paper

Experimental and Numerical Buckling Analysis of Carbon Fiber Composite Lattice Conical Structure before and after Lateral Impact

Ahmad Ahmadifar[1], Mohammad Reza Zamani[2], Ali Davar[3], Jafar Eskandari Jam[4] Mohsen Heydari Beni[5]

[1] M.Sc. Student, Mechanical Engineering Department, Malek-Ashtar University of Technology, Tehran, Iran
[2] Assistant Professor, Mechanical Engineering Department, Malek-Ashtar University of Technology, Tehran, Iran
[3] Assistant Professor, Composite Research Centre, Malek-Ashtar University of Technology, Tehran, Iran
[4] Professor, Mechanical Engineering Department, Malek-Ashtar University of Technology, Tehran, Iran
[5] Ph.D. Student, Mechanical Engineering Department, Malek-Ashtar University of Technology, Tehran, Iran

Received June 21 2019; Revised September 01 2019; Accepted for publication September 01 2019.
Corresponding author: M.R. Zamani (a_mrzamani@mut.ac.ir)

Abstract. In this research, the numerical and experimental analysis of the carbon fiber composite lattice conical structure has been performed to assess the buckling stability of the structure before and after the lateral impact. In the experimental analysis, the carbon fiber composite lattice conical structure was constructed with the winding method and using elastic molds and metal mandrel. In order to investigate the buckling stability of the structures before each lateral impact, they are subjected to be compressive-axial loading. The rest of the structures first subjected under the axial-compressive loading, then in the next step, a compressive loading is applied to determine the effect of the impact on the compressive strength of the damaged structures. In the numerical analysis, the Abaqus software is used to modeling and performing the mentioned analysis. Finally, the comparison of the results shows that the effect of the lateral impact causes how many reductions will be occurred in the buckling strength. So, it should be considered during the design of the applied structures. On the other hand, the low difference between the numerical and experimental simulations shows that the experimental and numerical methods can be used to analyze the structures with different geometric characteristics and material.

Keywords: Carbon fiber composite lattice conical structure, Experimental and numerical analysis, Lateral impact, Buckling analysis.

1. Introduction

Structural engineers to satisfy the common needs of different fields should have special characteristics and knowledge. The progress of an engineering project depends on the designer's understanding of the structure in order to solve the advanced challenges. With the entrance of composite materials into the technology world, the idea of constructing composite structures was expressed due to the strength and stability of these structures against metal structures. In this regard, various methods for constructing composite materials are invented. A total of these efforts resulted in the construction of new structures takes happened, which is called the composite lattice structure. These structures are a set

Published online: October 20 2019

of connected various fibers. Composite lattice structures due to their high strength and stiffness in comparison to their weight, today are widely used in various industries, especially in construction of aerospace structures, marine structures, etc. Composite lattice structures are one of the most advanced types of composite structures, and some of them are analyzed in this research. Previous studies on composites have shown that many composite structures are weak at lateral loading, which is provided an overview of the construction of lattice structures. In 2018, Ahmadifer et al. reviewed the influence of lateral impact on the buckling strength of composite lattice conical structures, which made of the glass-fiber. The results from this study shows that in the glass fiber-reinforced structures, the effect of the lateral impact significantly reduces the maximum structural strength in compressive-axial loading [1]. The first finite-element modeling and buckling analysis of the lattice conical shell subjected to axial loading, which has been done by Hou and Gramol [2]. Also, buckling analysis of the anisogrid conical spacecraft adapter subjected to combine (axial-compressive and bending) loading has been performed by Vasiliev et al [3]. The review of the buckling solutions obtained for the lattice cylindrical shells using continuum models as well as finite-element methods can be found in Morozov's article [4].

Considering the Re-modified Couple Stress Theory, Z. Yang and et al [5] added the Refined Zigzag Theory to the vibration and buckling analysis of sandwich micro-plates embedding FG layers. They show it for, two kinds of FG sandwich micro-plates with simply supported boundary conditions, which the present model can make precise estimates on those types of micro-structures by location the two orthogonal material length scale parameters equal to each other. Furthermore, Gao and et al [6] presented an adaptive continuation method for topology optimization of continuum structures considering buckling constraints. Meanwhile, Numerical examples were presented to illustrate the effectiveness of the proposed method. Lin and et al [7] investigated the vibration specifications and nonlinear aeroelastic response of the FG multilayer composite plate reinforced with graphene nanoplatelets subjected to in-plane excitations and applied voltage. In this study, based on high-order shear deformation theory, the motion equations of the FG plate system considering the Von-Karman geometric nonlinearity is derived using Hamilton's principle. The results showed that a small amount of graphene nanoplatelets (GPLs) reinforcement can have a substantial improvement effect on the performance of the composite plate structure. Emad Hasrati and et al [8] performed using an efficient numerical strategy, the nonlinear forced vibration analysis of composite cylindrical shells reinforced with single walled carbon nanotubes (CNTs). In this investigation, the governing equations are presented based on the first-order shear deformation theory along with Von-Karman nonlinear strain-displacement relations, and the results shown that the changes of central vibrational mode shape have considerable effects on the frequency response curves of composite cylindrical shells reinforced with CNTs. Pouresmaeeli and et al [9] investigated the static instability of functionally graded carbon nanotube-reinforced composite (FG-CNTRC) beam in the presence of the material and geometrical uncertainties. Ye Tang and et al [10] presented a novel model of fluid-conveying nanotubes made of bi-directional FG materials for investigating the dynamic behaviors and stability. In this study, based on Euler–Bernoulli beam and Eringen's nonlocal elasticity theories, the governing equation of the nanotubes and related boundary conditions are developed using Hamilton's principle. The results shown that the 2D material's distribution can meaningfully change the crucial flow velocity, essential frequencies and stability. Tomar and et al [11] investigated the thermo-mechanical buckling response of skew FG laminated plates with initial geometric imperfections. In this study, the formulation has been performed using Reddy's higher-order shear deformation theory (HSDT) with C^0 continuous displacement field. AKBAS in a study [12] to make the analysis of post-buckling of laminated composite beams under hygro-thermal effect concentrated. The novelty of this study is to investigate the hgyro-thermal post-buckling analysis of laminated composite beams by using the total Lagrangian nonlinear approach. The results showed that, fibber orientation angles, stacking sequence of laminas plays an important role in hygro-thermal post-buckling responses of laminated beams.

Davar and et al [13] in 2016 examined structures of reinforced composite lattice conical with and without carbon nanotubes under compressive-axial loading by both experimental and numerical analysis. In 2016, Zamani [14] investigated composite lattice structures with two experimental and numerical methods. In this research, the variety of composite lattice structures with two types of reinforcing grids having geometric patterns consisting of triangular and hexagonal grids, in two types with and without shells, were investigated. In 2015, Gerami [15] investigated the lateral impact influence on the buckling of the cylindrical lattice structures made of Kevlar fibers/epoxy with experimental and numerical methods. The results from this study shows that the free-drop damage in the reinforced lattice structures made of Kevlar fibers/epoxy due to the high absorption of energy by this fiber can't significantly reduce the maximum structural strength in compressive-axial loading. In the present study, the low difference between numerical and experimental simulations (In each of the three tests, including: buckling before lateral impact, lateral impact loading and buckling after lateral impact) indicate that the experimental and numerical methods created in this study, can be used to analyze structures of this type with different geometric characteristics and material, to save time and cost.

2. Structural Geometry Characteristic and Grid

The structures consist of: two non-shell structures of composite lattice conical, which made of carbon, and also each of the structures consists of ten pairs of spiral reinforcements and four peripheral reinforcements. The set of these spiral and peripheral reinforcements creates a geometric grid consisting of hexagonal cells in the overall configuration. In order to introduce the geometry of these structures, certain parameters have been used, which are presented in Table 1. For these structures.

Table 1. Geometric characteristics of the structure and grid of this research.

Type of characteristics	Characteristics	Symbols	Value
Grid geometric characteristics	Spiral reinforcements angle	Φ(degree)	28.2
	Thickness of the grid layer	H(mm)	6
	Peripheral reinforcements width	b_c(mm)	6
	Spiral reinforcements width	b_h(mm)	6
	Distance between Peripheral reinforcements	a_c(mm)	55.5
	Distance between Spiral reinforcements	a_h(mm)	64
Structure geometric characteristics	Small radius of Structure	R_1(mm)	140
	Large radius of Structure	R_2(mm)	170
	Structure height	L(mm)	163.2

3. Buckling Analysis of Structures before Lateral Impact

In this section, the buckling test results of the structure before the lateral impact are presented with numerical and experimental methods.

3.1. Numerical simulation of compressive-axial loading

Buckling loading analysis was carried out in this nonlinear simulation. The software used for this simulation was ABAQUS finite-element and simulation was done with shell elements. The reason for selecting the shell element is that in addition to the higher speed of analysis, the choice of this type of element allows the use of Hashin composite damage theory. Since the nature of the composite material is isotropic transversely, it is necessary to define the proper orientation for the structure in the ribs so that, the axis 1 of the composite material (Fiber direction) to be in the rib's direction. Initially, the geometric model of the composite lattice truncated cone is created into the software. Next, the material properties in the software is inputted. The elastic properties of glass/epoxy composites are also presented in Table 2. For structure meshing, totally number of 13460 elements S4R shells were applied. According to the mesh convergence graph (Fig. 1), these numbers of elements are suitable for the accuracy of the results as well as for the time of analysis. The boundary conditions applied in this simulation are the same as the experimental test, namely the insertion of two rigid plates in the upper and lower of the structure, and also the degrees of the freedom for the lower-plate are closed in the software, while the upper-plate allowed to move in the axial direction. To simulate the compressive-axial loading test of the structure, the type of analysis was chosen dynamically/explicit. The time required for the analysis should be such that, in addition to avoiding the very long time required for the software to be analyzed, large enough that the kinetic energy in the comparison with the energy stored in the whole structure to be insignificant. To avoid the entrance of nonlinear contact components and to increase the speed of problem-solving, the friction between the supports and structures has been neglected. To simulate carbon nanotube-reinforced composite lattice truncated cone, first, the properties of materials for different weight percentages of carbon nanotubes, using the micromechanical relationship (1) it was calculated and then entered into the simulation process.

$$\frac{E_c}{E_m}=\frac{1+(\zeta)(\frac{\frac{6E_f}{E_m}+1}{\frac{6E_f}{E_m}+\zeta})(V_f)}{1-(\frac{\frac{6E_f}{E_m}+1}{\frac{6E_f}{E_m}+\zeta})(V_f)}\qquad \zeta=\frac{2L}{D}e^{avf+b} \tag{1}$$

Table 2. Elastic properties for glass/epoxy composites

Mechanical Properties	Value
E_1 (Rib)	18 GPa
E_2	3.5 GPa
υ	0.3
G_{12}	1.4 GPa
G_{13}	1.4 GPa
G_{23}	1 GPa

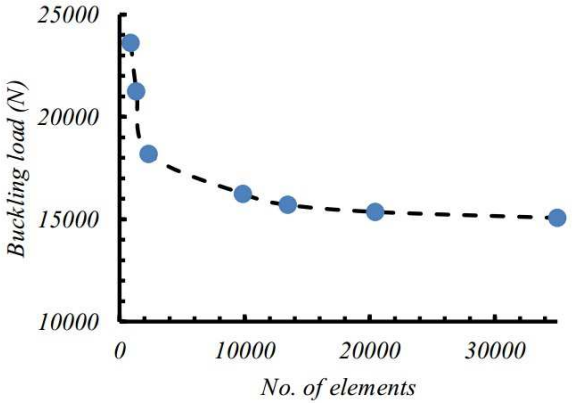

Fig. 1. Mesh convergence diagram

In Fig. 2, a numerical simulation model is presented in finite-element software. According to Fig.1, clearly the most critical points in the structure are at the intersection of the oblique reinforcements and the top of the last peripheral reinforcement, and the buckling of the structure occurs at these points. In Fig. 3, the force-displacement diagram is shown for the structure. According to Fig.3, the final buckling force is 40880.2 N, with the displacement of 3.53 mm.

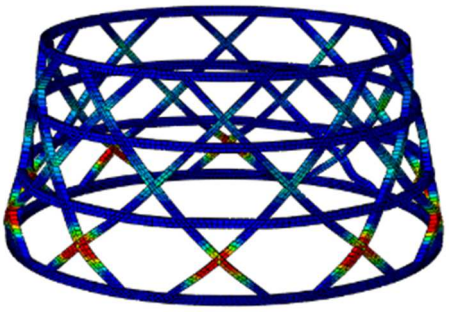

Fig. 2 Buckling numerical simulation before lateral impact.

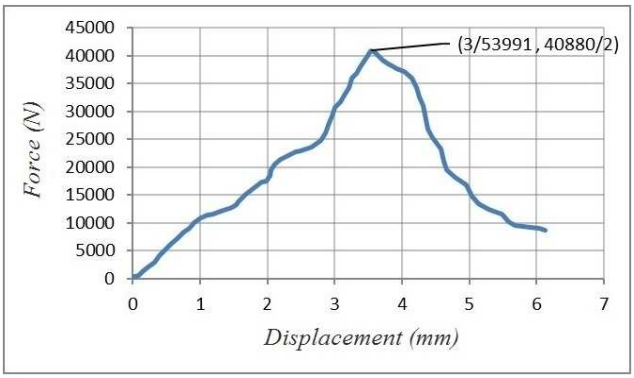

Fig. 3 Force-displacement diagram in numerical analysis under compressive-axial loading before the lateral impact.

3.2. Manufacturing of composite lattice truncated conical samples

Fig. 4 shows the geometrical model of the composite lattice truncated conical. The geometric parameters are presented in Table 3.

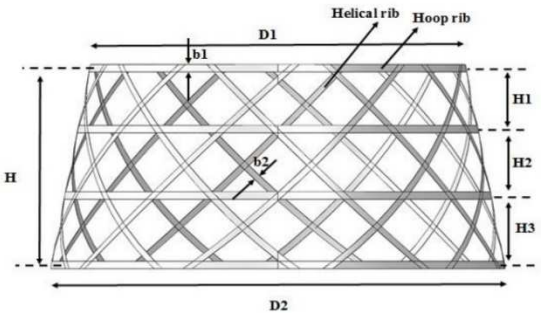

Fig. 4. Geometrical model for composite lattice truncated cone

Fig. 5. Metallic mandrel for composite lattice truncated cone

Fig. 6. Composite lattice truncated cone

Table 3. Geometrical parameters for composite lattice truncated cone

Parameters	Description	Value
D1	The outer diameter of the upper part	280 mm
D2	The outer diameter of the lower part	340 mm
H1	The upper part height	43 mm
H2	The middle part height	47 mm
H3	The lower part height	49 mm
H	Total height	166 mm
b1	Width of peripheral ribs	6 mm
b2	Width of spiral ribs	6 mm

Epoxy resin and glass fibers are used to manufacturing the test specimens. The fabrication of composite lattice truncated cone specimen was performed by fiber twisting method. Initially, the metal mold (mandrel) intended for fabrication is designed and fabricated according to the rib's arrangement in several parts. Fig. 5 shows the machining-step of mold prepared for fabrication. Next, the mold is placed on the twisting machine and the fabrication of the samples began. Resin Stained glass fiber inside the mold grooves is placed. And with the rotation of the mold, sample's manufacturing continued. To manufacturing carbon nanotubes sample; carbon nanotubes are first dispersed in the resin about %1 of own weight by the mechanical method and then reinforced resin with carbon nanotubes were used for the fabrication of lattice structures. Fig. 6 shows the samples made.

3.3. Experimental analysis results of compressive-axial loading

From the most important factors that make the results of experimental research reliable and accurate are the fact that the construction of the samples is carried out under the same conditions and with the same effective parameters in all specimens. In the constructed samples, the attempt was made to apply all of these parameters to the same samples and to

manufacture the samples with high precision, so that the results of the tests could be accurate and reliable.
After providing the necessary conditions for the test, the structures were arranged between the jaws of the system and the speed of applying the load was 0.5 mm per minute, that widespread uniform loading to the structure is carried out by relocation the moving jaw (in accordance with the quasi-static condition). At the same time, in the computer connected to the system, the force applied values to the structure were measured by the displacement of the jaw, and the corresponding diagram was depicted. In Fig. 7, the force-displacement diagram is shown for the structure. According to Fig.7, the final buckling force is 37833.3 N, with the displacement of 4.07 mm.
Also, in Fig. 8, the experimental buckling tests of the lattice conical structures are shown. According to the figures, after the failure occurred, the load is removed from the structures, so that the structures returned to their original condition, and somehow they did not appear to have seriously damaged and did not reach to have a complete failure.

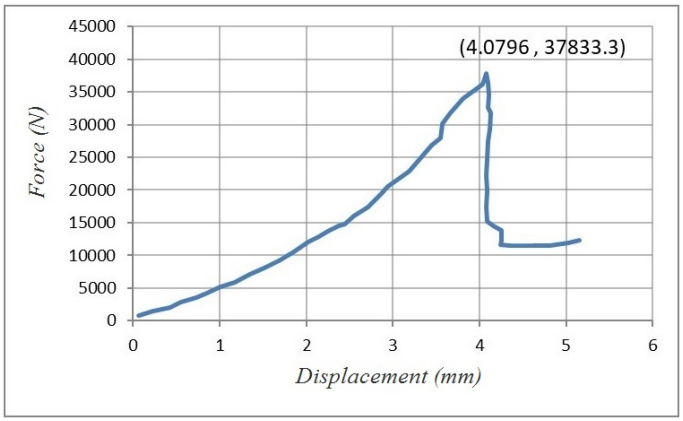

Fig. 7. Force-displacement diagram in experimental analysis of compressive-axial loading, before the lateral impact.

Fig. 8. Experimental analysis of compressive- axial loading, before the lateral impact.

3.3.1. Strength to weight ratio in structures

Considering the structure's weight and the results obtained from the structures buckling simulation, strength to weight ratio can obtain in composite lattice conical structures, which the results are presented in Table 4.

Table 4. The ratio of the buckling strength to structures weight

Type of analysis	Ratio of the buckling strength to structure weight (N/kg)
Experimental analysis	1.116×10^5
Numerical analysis	1.205×10^5
Average of Experimental & Numerical analysis	1.160×10^4

4. Results of Lateral Impact Analysis on the Structure

Since the main objective of the study is to investigate the lateral impact effect on the tolerable load amount in the composite lattice conical structures, the amount of impact that causes the damage to the structure is adequate. Therefore, there is not required to increase in the impactor mass amount or height (The collision moment speed) to create failure in the structure. It is worth noting that the mass of the impactor and the drop height were previously calculated using finite-element software.

4.1. Numerical simulation results of lateral impact

As stated above, the simulation of the finite-element of loadings has been done with the aid of ABAQUS software. In these simulations, the assumption "the rigidity of the spherical impactor, and the bottom plate of the structure," Was considered. In order to investigate and analyze the effect of lateral impact on the Maximum buckling bearable axial loading of the structure, in accordance with the experimental test, the impacts of 215.6 J into the structures by a mass-10kg from a height 2.02 meters, were applied. Using the relation v_2-v_{o2} = 2gh, the threshold velocity of the impactor's contact with the structure is calculated and the result is given to the software to allow the numerical simulation to be performed. The simulation of the impact done in the numerical analysis is shown in Fig. 9.

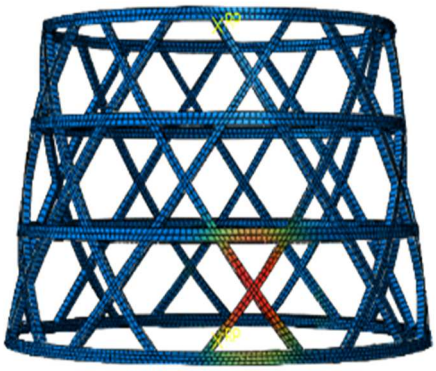

Fig. 9. Impact simulation in numerical analysis.

Fig. 10. Impact test in experimental analysis.

4.2. Experimental results of lateral impact

In this research, samples of constructs before the buckling test were first subjected to the lateral impact test. As shown in Fig. 10, each of these structures is placed inside the system and sent to each of the samples by sending command, that the spherical impactor to be dropped. Impactor mass is set at 10 kg for damage to structures. Furthermore, the drop height of the impactor was 2.20 m. After impacting the impactor to the structures, each of them is examined by the eye. As shown in Fig. 11, the damage caused by the impact on the structure, created cracks in it.
With closer attention to the structures after the lateral impact, it is seen that the structure at the impact location, as expected, was slightly broken and also white spots are created around it (indicating the breakdown of the resin). The damage around the impact point is almost symmetric.

Fig. 11. The impact location on the structure and the damage done.

5. The Axial Buckling Analysis after Applying Lateral Impact

The specimens, which are subjected to impact loading in the previous stage, at this stage applied a compressive-axial loading on them to determine the effect of impact on the compressive strength of the damaged structures.

5.1. Numerical simulation results of buckling after lateral impact

These simulations were performed in ABAQUS numerical analysis software in two steps. In the first stage, the lateral impact applied to the structure by an impactor with mass-5 kg and the speed 7 m/s. Then; in the second stage, the nonlinear analysis of the structure buckling was accomplished. In Fig. 12, a view of these simulations has been shown.
Furthermore, in Fig. 13, the force-displacement diagram is presented. This result from the numerical buckling analysis and using the ABAQUS software is achieved (after the lateral impact). According to this diagram, the final buckling force is 30354 N with a displacement of 3.64 mm.

5.2. Results of experimental buckling analysis after lateral impact

In Fig. 14, the force-displacement diagram is presented for the experimental buckling test under compressive-axial loading after the lateral impact. The movement speed of the jaw in this test similar to the experimental buckling test was 0.5 mm/min that according to numerical analysis. According to the results of this test, the maximum tolerated load in the structure the value %27.31 is reduced, compared to before the lateral impact (in the experimental analysis).
According to this diagram, the final buckling force is 27500 N, with a displacement of 4.43 mm. As shown in Fig. 15, the structures are failed from the area that they were impacted. Of course, the structure elsewhere also suffered damage such as cracking and breaking of the resin, but the greatest damage and the main failure at the impact location occurred.

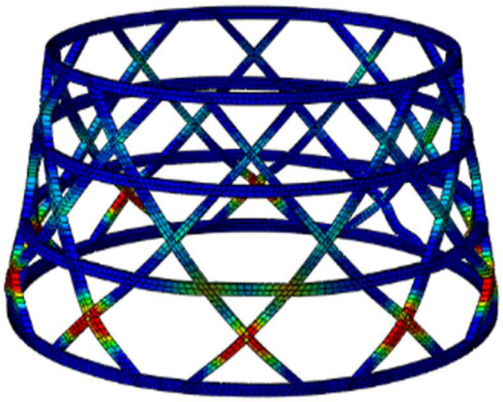

Fig. 12. Numerical simulation of buckling after lateral impact.

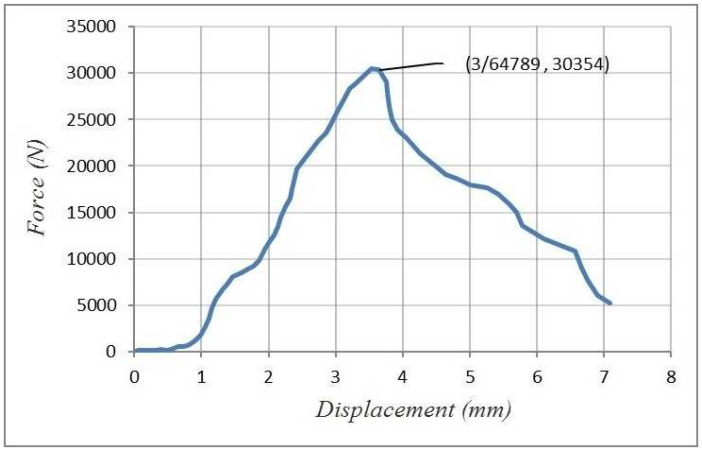

Fig. 13. Force-displacement diagram in compressive-axial loading numerical analysis, after the lateral impact.

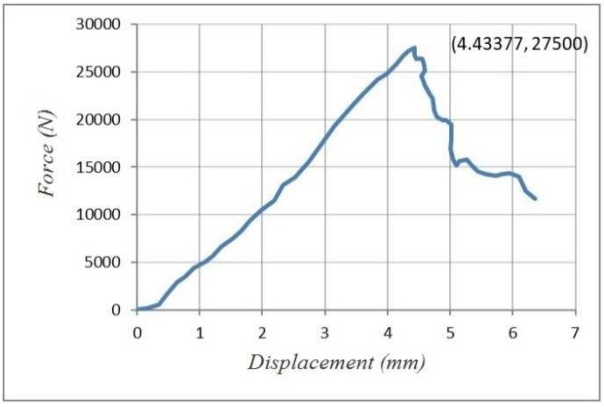

Fig. 14. Force-displacement diagram in experimental analysis of compressive-axial loading, after the lateral impact.

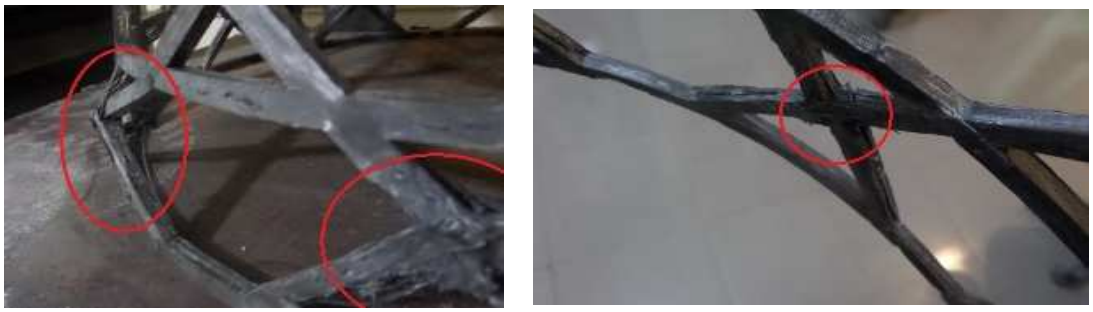

Fig. 15. Damages entranced to Structures in experimental analysis of compressive-axial loading, after the lateral impact.

6. Comparison of the Experimental and Numerical Analyses before and after Lateral Impact

In this section, the results of experimental and numerical analyzes in all loading are investigated and compared with each other. In the following figures, the force-displacement diagrams and area under these figures before and after the lateral impact were compared.

6.1. Comparison of numerical and experimental analysis results of tolerated force based on axial-displacement in structures

Regarding the values shown in Fig. 16 and 17, the results of the numerical and experimental analysis are very close together. Given that, the conditions in the manufacturing process always are not ideal and are accompanied by disadvantages and also, on the other hand, the modeling and analysis conditions are considered the ideal numerical design, the force tolerated value in numerical simulations is slightly greater than the corresponding experimental test results, which is predictable.

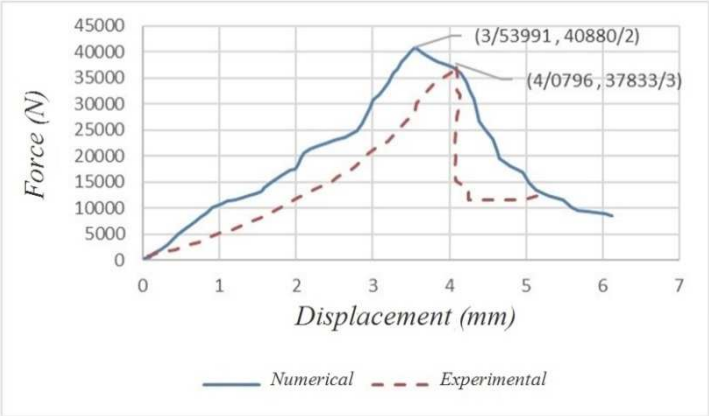

Fig. 16. Result's comparison of the numerical and experimental tests for compressive-axial loading before applying lateral impact.

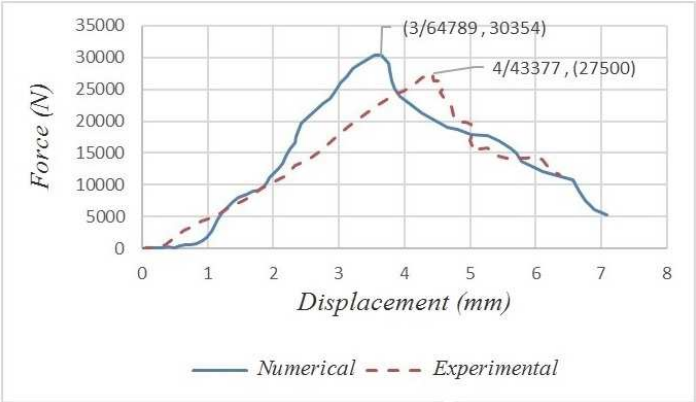

Fig. 17. Result's comparison of the numerical and experimental tests for compressive-axial loading after applying lateral impact.

6.2. Result's comparison of tolerated forces in according to axial-displacement in structures, before and after the lateral impact

As shown in Fig. 18 and 19, after the impact, the total axial-displacement is greater than the axial-displacement before the impact, which is due to the damage caused the impact on the structure. In fact, part of relocation caused that the cracks approached together and also caused damages from the impact. The comparison of the above diagram's result is presented in Table 5 in more detail. Regarding the obtained values, the lateral impact (on average in experimental and numerical analyzes) reduced the strength of the structure by 26.52%.

Table 5. Comparison of numerical and experimental results before and after lateral impact

Analysis Type	Buckling critical Load (N)		
	The difference Percent	After applying lateral impact	Before applying lateral impact
Experimental Analysis	27.31	27500	37833.3
Numerical Analysis	25.74	30354	40880.2
The difference Percent	26.52 (Average)	10.37	8.05

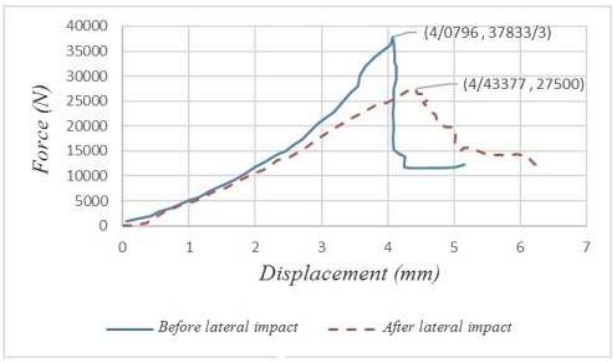

Fig. 18. Comparison of experimental buckling tests before and after lateral impact.

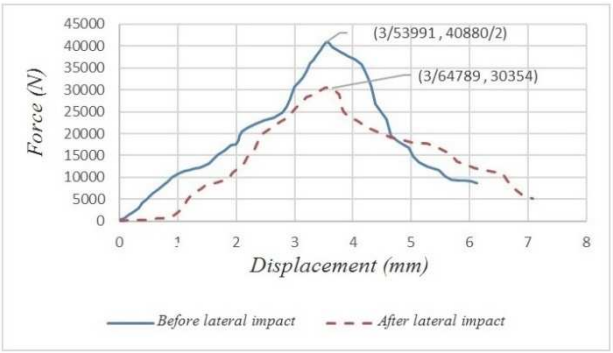

Fig. 19. Comparison of numerical buckling tests before and after lateral impact.

7. Conclusions

In the present study, the buckling stability of the structure before and after a lateral impact has been investigated. In the experimental analysis, the carbon fiber composite lattice conical structure are constructed with the winding method and using elastic molds and metal mandrel. In order to investigate the buckling stability of the structures before each lateral impact, each of the structures is subjected to be compressive- axial loading. Then, the other structures first are subjected under axial-compressive loading and in the next step, a compressive loading is applied to determine the effect of the impact on the compressive strength of the damaged structures. In the numerical analysis, the ABAQUS finite-element software is used for modeling and performing the mentioned analysis. In the end, the results from both methods used in this study are compared, and the results from these comparisons shows that effect of the lateral impact to each of the structures causes how many the reduction in the buckling strength, so that, it could be considered during the design of the applied structures. On the other hand, the low difference between the numerical and experimental simulations of this research shows that experimental and numerical methods can be used to analyze structures of this type with different geometric characteristics and material, and also to save time and cost.

Author Contributions

The manuscript was written through the equal contribution of all authors. All authors discussed the results, reviewed and approved the final version of the manuscript.

Conflict of Interest

The authors declared no potential conflicts of interest with respect to the research, authorship and publication of this article.

Funding

The authors received no financial support for the research, authorship and publication of this article.

References

[1] A. Ahmadifar, M.R. Zamani, A. Davar, *Numerical and experimental analysis of buckling in composite grid stiffened conical structures, with and without shell, before and after the transverse impact*, Master's Thesis Malek Ashtar University, Tehran, Iran, 2018. (in Persian)
[2] A. Hou, K. Gramoll, Compressive strength of composite latticed structures, *J. Reinf. Plast. Compos.*, 17(5), 1998, 462–83.
[3] V.V. Vasiliev, A.F. Razin, G. Totaro, F. De Nicola, *Anisogrid conical adapters for commercial space application*, In: AIAA/CIRA 13th international space planes and hypersonics systems and technologies, 16–20 May, Centro Italiano Ricerche Aerospaziali (CIRA) Capua, 2005.
[4] E.V. Morozov, A.V. Lopatin, V.A. Nesterov, Finite-element modelling and buckling analysis of anisogrid composite lattice cylindrical shells, *Compos. Struct.*, 93, 2011, 308–323.
[5] Z. Yang, D. He, Vibration and Buckling of Functionally Graded Sandwich Micro-Plates Based on a New Size-Dependent Model, *Int. J. Appl. Mech.*, 11(1), 2019, 1950004.
[6] X. Gao, L. Li, H. Ma, An Adaptive Continuation Method for Topology Optimization of Continuum Structures Considering Buckling Constraints, *Int. J. Appl. Mech.*, 9(7), 2017, 1750092.
[7] H.G. Lin, D.Q. Cao, Y.Q. Xu, Vibration, Buckling and Aeroelastic Analyses of Functionally Graded Multilayer Graphene-Nanoplatelets-Reinforced Composite Plates Embedded in Piezoelectric Layers, *Int. J. Appl. Mech.*, 10(3), 2018, 1850023.
[8] E. Hasrati, R. Ansari, J. Torabi, Nonlinear Forced Vibration Analysis of FG-CNTRC Cylindrical Shells Under Thermal Loading Using a Numerical Strategy, *Int. J. Appl. Mech.*, 9(8), 2017, 1750108.
[9] S. Pouresmaeeli, S.A. Fazelzadeh, Uncertain Buckling and Sensitivity Analysis of Functionally Graded Carbon Nanotube-Reinforced Composite Beam, *Int. J. Appl. Mech.*, 9(5), 2017, 1750071.
[10] Y. Tang, T. Yang, Bi-Directional Functionally Graded Nanotubes: Fluid Conveying Dynamics, *Int. J. Appl. Mech.*, 10(4), 2018, 1850041.
[11] S.S. Tomar, M. Talha, Thermo-Mechanical Buckling Analysis of Functionally Graded Skew Laminated Plates with Initial Geometric Imperfections, *Int. J. Appl. Mech.*, 10(2), 2018, 1850014.
[12] S.D. Akbas, Hydrothermal Post-Buckling Analysis of Laminated Composite Beams, *Int. J. Appl. Mech.*, 11(1), 2019, 1950009.
[13] A. Davar, R. Azar Afza, V. Bagheri, *Experimental and numerical analysis of composite lattice truncated conical structures with and without carbon nanotube reinforcements under axial compressive force*, Master's Thesis Malek Ashtar University, Tehran, Iran, 2019. (in Persian)
[14] M.R. Zamani, M.R. Khalili, *Numerical And Experimental Transient Dynamics Analysis for Cylindrical Composite Lattice Structure*, Ph.D. Thesis KhajeNasir University, Tehran, Iran, 2016. (in Persian)

[15] A. Gerami, M.R. Zamani, *Theoretical and Experimental Buckling Analysis of Grid Stiffened Cylindrical Shells Before And After Applying Transverse Impact*, Master's Thesis Malek Ashtar University, Tehran, Iran, 2015. (in Persian)

ORCID iD

Ali Davar https://orcid.org/0000-0002-4386-1965
Jafar Eskandari Jam https://orcid.org/0000-0002-4888-3071